

Deep Learning for Model-Free Prediction of Thermal States of Robot Joint Motors

Trung Kien La * Eric Guiffo Kaigom *

* Department of Computer Science & Engineering, Frankfurt University of Applied Sciences, 60318 Frankfurt am Main, Germany (e-mails: trung.la@stud.fra-uas.de; kaigom@fb2.fra-uas.de).

Abstract: In this work, deep neural networks made up of multiple hidden Long Short-Term Memory (LSTM) and Feedforward layers are trained to predict the thermal behavior of the joint motors of robot manipulators. A model-free and scalable approach is adopted. It accommodates complexity and uncertainty challenges stemming from the derivation, identification, and validation of a large number of parameters of an approximation model that is hardly available. To this end, sensed joint torques are collected and processed to foresee the thermal behavior of joint motors. Promising prediction results of the machine learning based capture of the temperature dynamics of joint motors of a redundant robot with seven joints are presented.

Keywords: Robotics, Artificial Intelligence / Machine Learning, Temperature Management.

1. INTRODUCTION

Robots are commonly used to achieve repetitive and hazardous tasks in industry and society. Meanwhile, they increasingly and skillfully assist and augment humans. Included are applications with a pronounced level of physical interactions between humans and robots, such as using a robot as a companion (Basha (2025)), home-helper and caregiver (Tsui et al. (2025), Gkolonta et al. (2025)), as well as a prosthesis (Kim et al. (2025)). In this respect, high payload manipulations, large joint accelerations, and motions with specific configurations (see, e.g., Fig. 1) can induce the overheating of joint motors of robots. Excessive motor temperatures are detrimental in many ways. They can accelerate the degradation of insulation materials and reduce motor efficiency (Yehorov et al. (2025)) along with jeopardizing the positioning accuracy of the robot due to axial deformations and drifts (Soga et al. (2024)).

Most robot manufacturers, including Franka, Kinova, and KUKA, offer built-in functions to shut down the robot once a critical temperature threshold is attained. Whereas this functionality is advantageous to preserve the performance and reliability of motors and surrounding electronic components, an undesired shutdown tends to compromise the robot availability for production and assistance purposes. This situation gets exacerbated as the robot is not equipped with mechanical brakes, as in Fig. 1. In this case, critical collisions with the environment might occur, endangering human beings or leading to hardware (i.e., robot, workpiece, workcell, etc) damages. Furthermore, thermal burns represent not only a severe safety issue in physical human-robot-interaction, but also a hindrance for elevated user experience that is necessary to engage and sustain a symbiosis between humans and robots. Predicting the thermal behavior of robot joints is therefore an essential step toward the development of countermeasures that help anticipate overheating, preserve the robot avail-

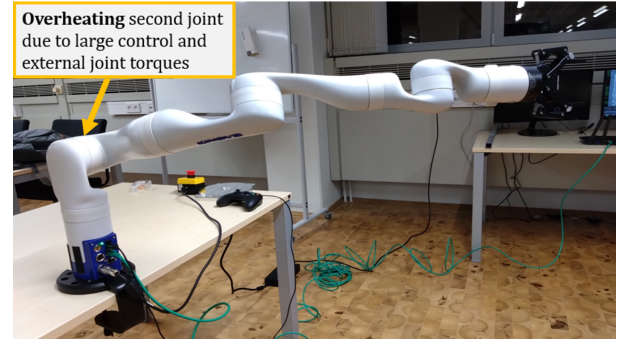


Fig. 1. Posture increasing the temperature of the 2. motor.

ability, prolong its lifetime, and improve its usability. Industry 4.0, industry 5.0, together with society 6.0 are likely to benefit from this capability. In fact, the thermal prediction propels operational efficiency through its significant contribution to the design of thermally uncritical trajectories that preserve the motor performance and thus robot availability in fully automated high-speed low-time-to-market manufacturing. This skill is missing in current industrial applications. Endowing robots with a thermal management based upon machine learning is useful to accommodate uncertainties emanating from *unseen* events. These include the highly dynamic robotized human-centered assistance for smart living and social well-being. These goals require an approach that turns robot diversity and application uncertainties into competitive advantages in terms of flexibility, transferability, and scalability.

This work predicts the thermal behavior of joint motors. The prediction approach is

- data-driven, paving the ground for an insightful, non-invasive, and inclusive operationalization in real-time.
- model-free through the development of a deep learning-based framework that leverages multiple hybrid layers to capture the unknown dynamics between

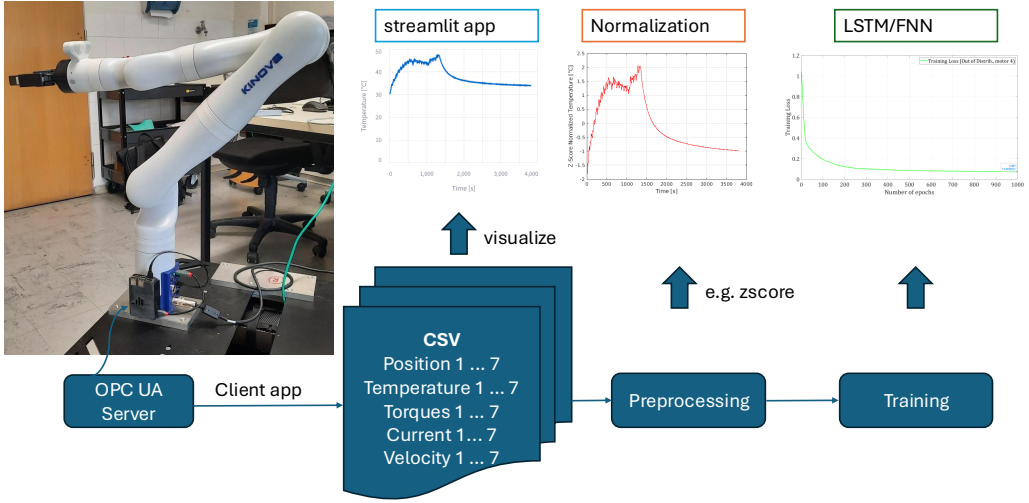


Fig. 2. Data collection from the Kinova robot (l.h.s) via an OPC UA Server and simplified processing pipeline (r.h.s).

joint actuation and motor temperature. No system-related parametric or actuation profile assumptions are made. Model complexity is thereby avoided. Generalization to new events and transferability to other robot types regardless of the number and type of joint motors are fostered.

- evaluated on data collected from a redundant Kinova Gen 3 robot with seven joints (see Fig. 2). Practical advantages of data normalization are highlighted.

2. RELATED WORK

Predicting the temperature behavior of robot motors has attracted attention in the recent years. Afaq et al. (2023) focus on thermal management of robotic applications under extreme temperatures. Electronics heating and cooling are considered. A temperature control driven by fuzzy logic is developed and demonstrated to this end. Decreases of extreme high temperature from 50° to 8° are shown. Fan-based forced convection is used to cool electronics. Excessive internal temperatures in a permanent magnet synchronous motor (PMSM) taking non-stationary loads, which might lead to a reduction of its life time, is addressed in Chen et al. (2024). An accelerated degradation model is derived to evaluate the reliability function and predict the lifetime of the PMSM under thermal stress. Geometric backlash and temperature-related drift errors in joints of industrial robots are compensated in Sigror et al. (2023). A model that reflects the thermal expansion of links is developed and used for thermal expansion correction. LSTM Neural Networks (He et al. (2024)) and Pseudo-Siamese Nested LSTM (Cai et al. (2021)) are employed to predict the temperature in Permanent Magnet Synchronous Motors. A trapezoidal torque profile is employed in He et al. (2024) whereas the torque dynamics is not released in (Cai et al. (2021)). A thermal recovery of robot joints is achieved in Jorgensen et al. (2019). To this end, the thermal dynamics is captured as a first order ordinary differential equation subject to constant positive and negative step-like profiles of joint torques. The exponential-

based dynamics of the temperature behavior is derived. A parameter identification is carried out to demonstrate the performance of the model for step-like joint torques.

Contributions mentioned thus far are mostly model-driven. They fit with specific robots provided that parameters have been identified in advance. However, parameter identification requires noise robustness and low sensitivity (Zhang et al. (2024), de Hoyos Fernández de Córdova et al. (2024)), which is a time consuming analysis task prone to additional uncertainties due to unseen/unmodeled/truncated dynamics (Shang et al. (2024)). Sometimes, such a process must be repeated from scratch for a given new robot, which inhibits quick and large scale automation involving multiple robots in terms of complexity, workload, and costs. As the robot is hardly accessible, such as in space servicing, identification tasks might be hard to complete because of limited access to pertinent (e.g., excitation) data. Autonomous task completion without human interventions, as expected by Industry 6.0, calls for machine learning-embedded solutions (Carayannis et al. (2024)) that can extend the robot skills for self-condition monitoring. The approach proposed in this work also falls into this category. Robot datasets available from standard APIs are harnessed to predict the thermal behavior of its joint motors. Trained machine learning models can be run by services of digital twins (see Kaigom (2023) and Kaigom and Roßmann (2020)) with which the physical robot is embedded to detect and anticipate detrimental thermal issues. In contrast to related works, no restriction is made on robot types, number of joints, and actuation profiles.

3. METHOD

3.1 System overview

The full state of our experimental Kinova Gen 3 ultralightweight robot with seven degrees-of-freedom (Kinovarobotics (2025)) is recorded using a specially developed OPC Unified Architecture server (Girke et al. (2024)). Positions, temperatures, torques, velocities and currents

of each of the seven joints are stored, via a client application, as parameters in CSV files and subsequently processed for the neural network trainings, see Fig. 2. To cover a wide range of robotic movements, both randomly generated joint angle trajectories and predefined Cartesian trajectories for pick and place tasks, for example, are generated using the Kortex API (Robotics (2025)). The trajectories are initially tracked at varying speeds and with different payloads. The recording duration of each set of trajectories is also varied in order to analyze the temperature rise and the cooling behaviour of the joints. For cooling, the robot was positioned in a vertical position, as this joint configuration imposes minimal load torques on the joints. Movements without intentional cooling are also conducted sequentially to include as realistic and diversified conditions as possible. Randomized joint position are constrained within minimum and maximum limits to avoid potential collisions with the environment. Completed experiments indicate that the second and fourth joint exhibit the highest temperature increases.

3.2 Temperature profile approximation

The temperature profile can be represented approximately with the Gaussian model (i.e. Gauss2) as shown in Fig. 3 and outlined in eq. (1):

$$f(x) = a_1 \cdot \exp \left(-\left(\frac{x - b_1}{c_1} \right)^2 \right) + a_2 \cdot \exp \left(-\left(\frac{x - b_2}{c_2} \right)^2 \right) \quad (1)$$

Coefficients and metrics for the profile in Fig. 3 are:

$$a_1 = 34.07, \quad b_1 = 276, \quad c_1 = 743.2, \\ a_2 = 1.668, \quad b_2 = -26.71, \quad c_2 = 103$$

Root Mean Squared Error (RMSE): 0.081294
 R^2 (coefficient of determination): 0.9897

Although the Gauss2 approximation is accurate, it has some limitations. The coefficients vary for each temperature profile and must be recalculated. Neural networks offer a more generalizable and robust approximation.

3.3 Feedforward and LSTM neural networks

Feedforward neural networks (FNN) shift data from the input to the output of a neural network. Backpropagation is run to optimize the neural weights. FNN have a simplistic structure and are limited in their ability to incorporate past values. Recurrent neural networks (RNN) therefore have feedback loops to store past values via hidden states. This allows them to understand long-term dependencies, which results in more stable predictions. However, RNNs lose old information over time. With LSTMs, long-term information is stored more effectively. They feature cell state for long-term memory and hidden state for short-term memory. In addition, the storage and removal of information is controlled via four gates (Input Gate, Forget Gate, Cell Gate, Output Gate). They are therefore used for predictions where a large number of past states have an influence on future states (Ljung et al. (2020)).

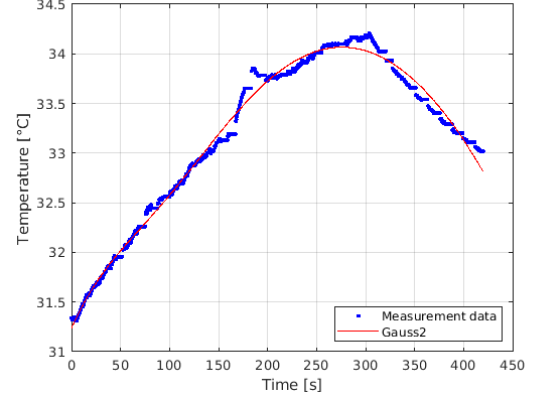


Fig. 3. Approximation of the temperature profile of the 4th joint with the Gauss2 function.

Table 1 compares neural networks integrated in this work to benefit from their respective strengths. In essence,

- FNNs disregard historical information and consider each input independently. LSTM networks are able to store the context of previous points in time (sequential data) through memory cells and use this information for future predictions (Liu et al. (2019)).
- FNNs can be trained with lower computational power and in a shorter time compared to LSTMs, which consists of more complex structures (e.g., states and gates). LSTMs store and update past information.
- Joint temperatures change as a result of continuous loads and the temporal dynamics of joint torques. The time-dependency can be captured by LSTMs. They are specifically designed for time series. FNNs are more suitable for regression problems on static data points where a disturbance or modifying of the temporal dynamics is non-critical.

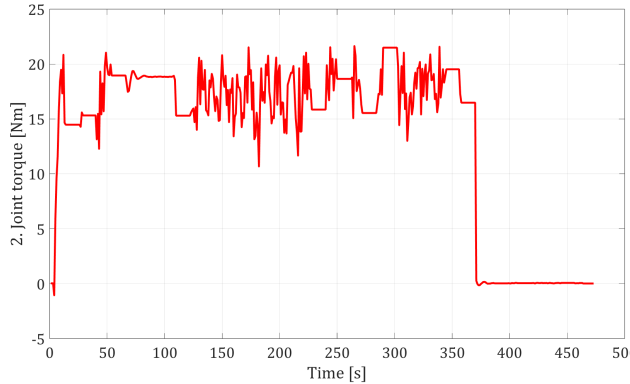
We implement and train a deep neural network that combines LSTM as a feature-extractor for time series dependencies in the input torque data and multiple Feedforward layers to take advantage of the extracted features for the subsequent temperature prediction at the network output.

4. APPLICATION

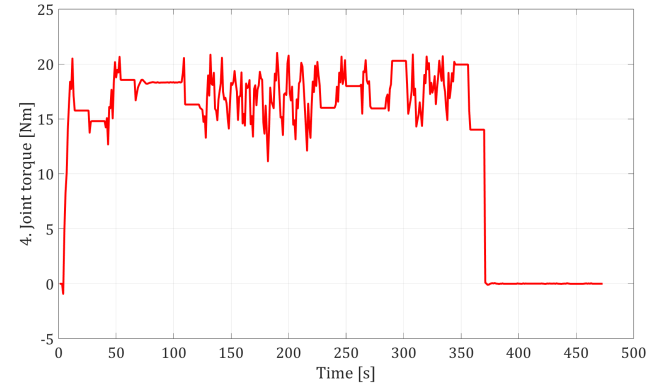
Experiments have been carried out to predict the temperature of all the seven joint motors of the robot in Fig. 1 by using joint torques and without any information about how the joint torques map to motor temperatures and any assumption on the joint torque profiles. Another goal impacting the energy autonomy was to keep training data for a satisfactory prediction accuracy small. We target remote use cases with on-board intelligence in the future.

Table 1. Comparison between Feedforward and LSTM neural networks

Feature	FNN	LSTM
Handles Sequential Data	No	Yes
Computational Complexity	Low	High
Training Time	Fast	Slow
Memory Requirements	Low	High
Suitable for Static Inputs	Yes	No
Suitable for Time-Series Data	No	Yes

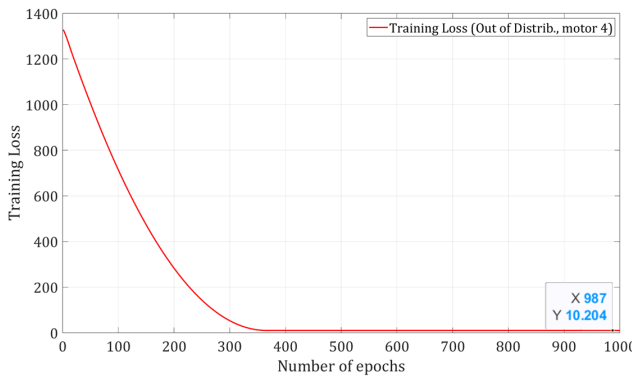


(a) Torque profile of the 2. motor.

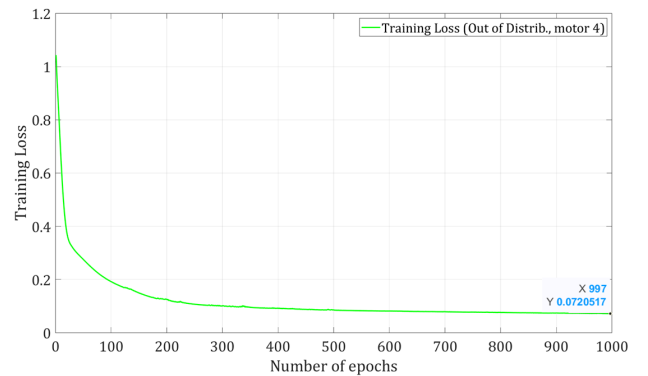


(b) Torque profile of the 4. motor.

Fig. 4. Two different non-trivial torque profiles of the robot in Fig. 1. Observe that the profiles go beyond step functions.



(a) Training loss without data normalization.



(b) Training loss with z-score data normalization.

Fig. 5. Enhanced convergence velocity and effectiveness of the training loss through data normalization.

4.1 Data collection and pre-processing

The collected datasets allow the utilization of joint positions, torques, velocities, and currents of all seven joints as input features. The selection of the input values for the training can be adjusted as needed, varying from 7 to a total of 28 inputs (Fig. 2). However, the best result was observed with only the joint torques (see Fig. 4) as input features for the neuronal network. The temperature values of the seven joints are used as targets. To evaluate the temperature predictions from the neural networks, randomly selected temperature measurements serve as ground truth.

The setup for collecting joint torques and corresponding motor temperatures is shown in Fig. 2. Recorded profiles of joint torques are rather challenging when compared to step profiles considered in related works. Acquired data are not filtered. A z-score normalization of input (i.e., joint torques) and target (motor temperatures) data is carried out before training. The mean μ and standard deviation σ of target temperature data from the normalization are stored. After training, the original temperature data x is reconstructed from the predicted \tilde{x} according

$$x = \tilde{x}\sigma + \mu \quad (2)$$

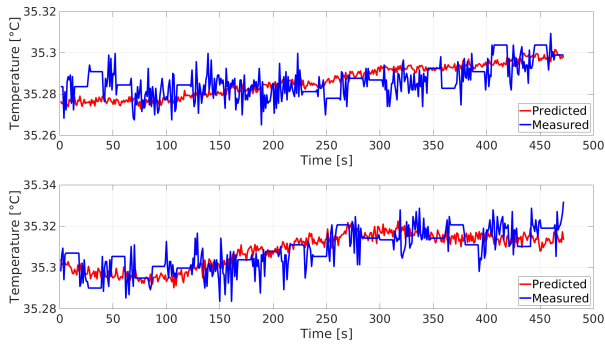
Data normalization has significantly sped up the training process and enhanced the prediction accuracy (see Fig. 5).

4.2 Model training

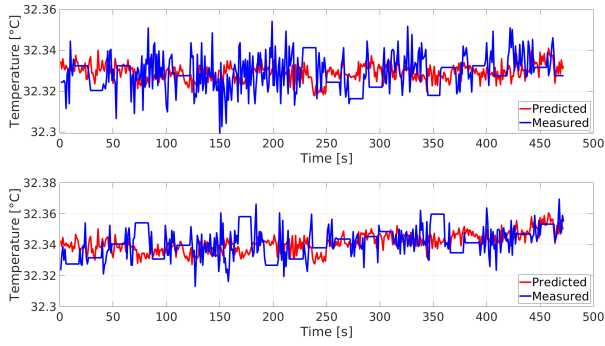
The mean squared error between network output and target temperature data is adopted as loss function. Back propagation is leveraged for the gradient-based optimization of network weights. The Adaptive Moment Estimation adapts the learning rate. The probability with which input elements are dropped out (i.e., set to zero) to prevent network over-fitting is set to 0.1. A mixture of *tanh*, *elu*, and *sigmoid* are distributed as activation functions (a type per layer) to inject non-linearities into the network. The output layer activation is the identity function.

4.3 Prediction results

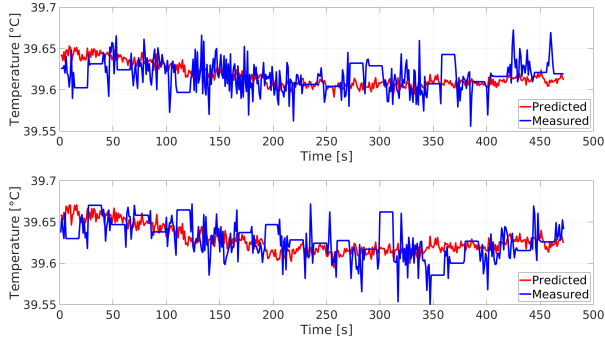
The trained neural network of seven hidden layers (one LSTM layer, six feed forward layers with a decreasing number of neurons toward the output) is fed with torque data. The network input is a dataset *unseen* during training. The goal is to assess the generalization capability of the network when facing new dynamics of the robot (Fig. 6). Two generalization tests are completed for each of the seven joints. An additional test with seen data is conducted and restricted to the second joint. Validation and generalization results are shown in Fig. 6. Table 2 summarizes the RMSE and the max. absolute error (MaxAE) of the predictions. Whereas motor temperatures are predicted with negligible RMSE (below 0.17°) when the two seen datasets



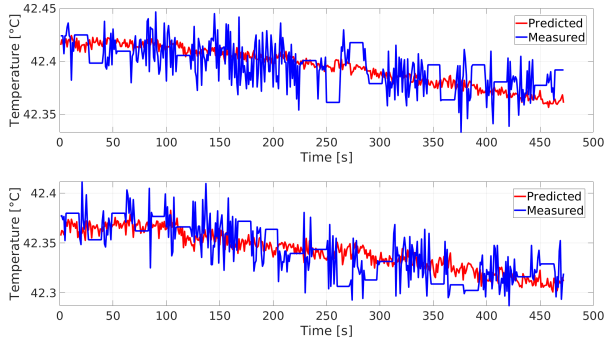
(a) Motor 1: Different predictions with **unseen** joint torques.



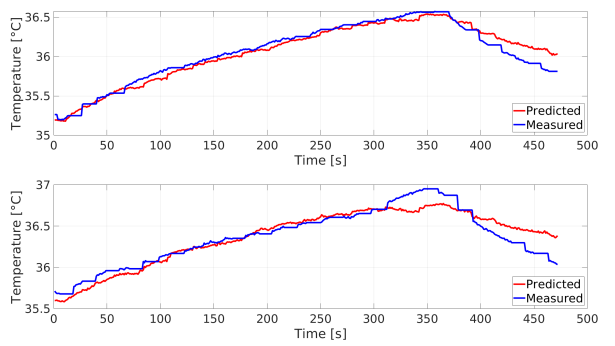
(c) Motor 3: Different predictions with **unseen** joint torques.



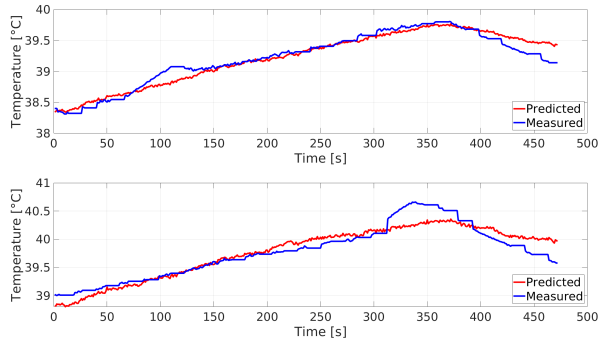
(e) Motor 5: Different predictions with **unseen** joint torques.



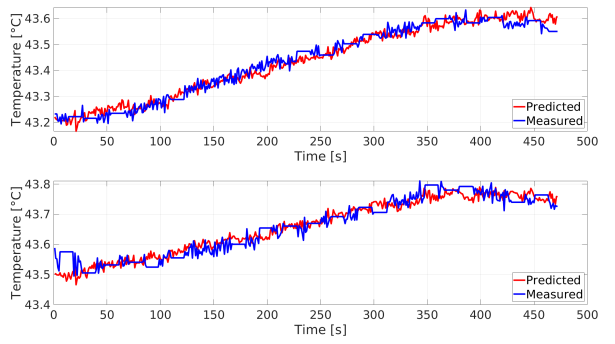
(g) Motor 7: Different predictions with **unseen** joint torques.



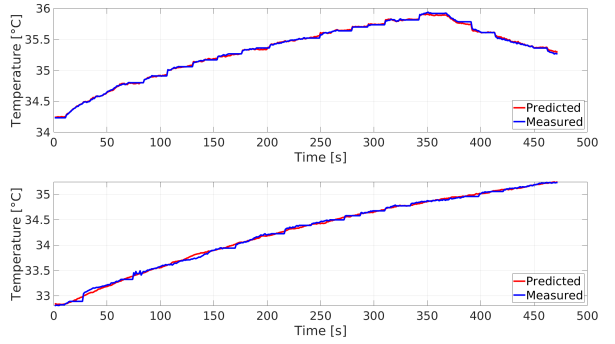
(b) Motor 2: Different predictions with **unseen** joint torques.



(d) Motor 4: Different predictions with **unseen** joint torques.



(f) Motor 6: Different predictions with **unseen** joint torques.



(h) Motor 2: Different predictions with **seen** joint torques.

Fig. 6. Capturing the thermal behavior of joint motors of the robot in Fig. 1 with previously unseen and seen data.

are used as inputs of the trained network (see Fig. 6.h), the absolute value of the overall prediction error remains below 0.5° in the case of totally unseen data (see Fig. 6.a-

g). It is worth noting that the small training dataset is randomly generated. Generalization accuracy can be further enhanced by augmenting the amount of training data.

Table 2. RMSE and MaxAE of Fig. 6 a-h. The first RMSE and MaxAE values refer to the upper, the second values refer to the lower plots of the respective motor temperatures.

Motor no.	RMSE [°C]	MaxAE [°C]
(a) Motor 1	0.0076 0.0068	0.0246 0.0224
(b) Motor 2	0.0853 0.1166	0.2674 0.3503
(c) Motor 3	0.0094 0.0105	0.0308 0.0274
(d) Motor 4	0.1054 0.1625	0.3327 0.4275
(e) Motor 5	0.0202 0.0209	0.0638 0.0826
(f) Motor 6	0.0259 0.0275	0.0762 0.0974
(g) Motor 7	0.0178 0.0188	0.0441 0.0535
(h) Motor 2 (seen)	0.0152 0.0290	0.0467 0.0911

However, an advantage of working on a small dataset is to assess how a minimum amount of data, energy demand, and a satisfactory accuracy relate. In our specific case, 16 datasets with recording time length as in Fig. 4 is suitable. Insights gained are useful to steer on-board machine learning in mobile robots under energy autonomy constraints.

5. CONCLUSION

This work shows that the temperature behavior of a robot can be predicted in advance without any analytical model about how joint torques map to motor temperatures. The proposed approach is not only model-free but also scales up for any number of joint motors and generalizes when exposed to unseen inputs despite the small amount of training data being used. Its effectiveness is evaluated and demonstrated for complex joint torque profiles and each of the seven joints of the experimental robot. The proposed framework can help anticipate and alleviate widespread shutdown of industrial and service robots once a critical temperature is attained, design thermally uncritical joint trajectories, prolong the lifetime of robot motors, and prevent thermal burns in industry and society.

REFERENCES

Afaq, M., Jebelli, A., and Ahmad, R. (2023). An intelligent thermal management fuzzy logic control system design and analysis using ansys fluent for a mobile robotic platform in extreme weather applications. *Journal of Intelligent & Robotic Systems*, 107(1), 11.

Basha, A.J. (2025). Robotic companions in healthcare: Investigate the role of humanoid robots in augmenting patient well-being.

Cai, Y., Cen, Y., Cen, G., Yao, X., Zhao, C., and Zhang, Y. (2021). Temperature prediction of pmsms using pseudo-siamese nested lstm. *World Electric Vehicle Journal*.

Carayannis, E.G., Posselt, T., and Preissler, S. (2024). Toward industry 6.0 and society 6.0: The quintuple innovation helix with embedded ai modalities as enabler of public interest technologies strategic technology management and road-mapping. *IEEE Transactions on Engineering Management*.

Chen, M., Zhang, B., Li, H., Gao, X., Wang, J., and Zhang, J. (2024). Lifetime prediction of permanent magnet synchronous motor in selective compliance assembly robot arm considering insulation thermal aging. *Sensors*, 24(12), 3747.

de Hoyos Fernández de Córdova, A., Olazagoitia, J.L., and Gijón-Rivera, C. (2024). Non-invasive identification of vehicle suspension parameters: A methodology based on synthetic data analysis. *Mathematics*, 12(3), 397.

Girke, F., Harmann, R., and Kaigom, E.G. (2024). Systems of digital twins and physical systems: Interoperability, decentralization, and mobility in robotic applications. *2024 28th International Conference on Methods and Models in Automation and Robotics (MMAR)*.

Gkiolnta, E., Roy, D., and Fragulis, G.F. (2025). Challenges and ethical considerations in implementing assistive technologies in healthcare. *Technologies*, 13(2), 48.

He, L., Feng, Y., Yan, Z., and Cai, M. (2024). Rotor temperature prediction of pmsm based on lstm neural networks. *Arabian Journal for Science and Engineering*, 1–12.

Jorgensen, S.J., Holley, J., Mathis, F., Mehling, J.S., and Sentis, L. (2019). Thermal recovery of multi-limbed robots with electric actuators. *IEEE Robotics and Automation Letters*, 4(2), 1077–1084.

Kaigom, E.G. (2023). Metarobotics for industry and society: Vision, technologies, and opportunities. *IEEE Transactions on Industrial Informatics*.

Kaigom, E.G. and Roßmann, J. (2020). Value-driven robotic digital twins in cyber-physical applications. *IEEE Transactions on Industrial Informatics*, 17(5), 3609–3619.

Kim, H., Lee, D., Maldonado-Contreras, J.Y., Zhou, S., Herrin, K.R., and Young, A.J. (2025). Mode-unified intent estimation of a robotic prosthesis using deep-learning. *IEEE Robotics and Automation Letters*.

Kinovarobotics (2025). Kortex api. <https://www.kinovarobotics.com/product/gen3-robots>. [Online; accessed 1-Feb-2025].

Liu, N., Li, L., Hao, B., Yang, L., Hu, T., Xue, T., and Wang, S. (2019). Modeling and simulation of robot inverse dynamics using lstm-based deep learning algorithm for smart cities and factories. *IEEE Access*.

Ljung, L., Andersson, C., Tiels, K., and Schön, T.B. (2020). Deep learning and system identification. *IFAC-PapersOnLine*, 53(2), 1175–1181.

Robotics, K. (2025). Kortex api. https://github.com/Kinovarobotics/Kinova-kortex2_Gen3_G3L. [Online; accessed 1-Feb-2025].

Shang, C., Yang, M., and You, J. (2024). A general parallel disturbance controller for pmsm drives based on frequency domain design. *IEEE Transactions on Industrial Electronics*.

Sigron, P., Aschwanden, I., and Bambach, M. (2023). Compensation of geometric, backlash, and thermal drift errors using a universal industrial robot model. *IEEE Transactions on Automation Science and Engineering*.

Soga, T., Hanai, H., Hirogaki, T., and Aoyama, E. (2024). Skillful operation of working plate for grasp less ball handling with an industrial dual-arm robot considering temperature of joint motors. *International Journal of Modeling and Optimization*, 14(4).

Tsui, K.M., Baggett, R., and Chiang, C. (2025). Exploring embodiment form factors of a home-helper robot: Perspectives from care receivers and caregivers. *Applied Sciences*, 15(2), 891.

Yehorov, A., Duniev, O., Masliennikov, A., Gouws, R., Dobzhanskyi, O., and Stamann, M. (2025). Study on the thermal state of a transverse-flux motor. *IEEE Access*.

Zhang, X., Cao, Y., and Zhang, C. (2024). Model predictive voltage control for pmsm system with low parameter sensitivity. *IEEE Transactions on Industrial El.*